Electronic Supplementary Material (ESI) for Nanoscale.
This journal is © The Royal Society of Chemistry 2017

Supporting Information

Controlled synthesis of lanthanide-doped Gd_2O_2S nanocrystals with a novel excitation -dependent multicolor emissions

Lei Lei, Shengjun Zhang, Han Xia, Ying Tian, Junjie Zhang, Shiqing Xu**

College of Materials Science and Engineering, China Jiliang University, Hangzhou 310018, P. R. China

Table S1 and Figure S1-S14

Table S1 the detailed conditions for synthesizing Gd_2O_2S NCs with different morphologies

	A : B : C	OA:OM:ODE	*T* [°C]	*t* [min]	Phase	Morphology	Mean-size [nm]
Gd_2O_2S	0 : 0 : 10	1 : 3 : 4	315	60	hexagonal	plate	~7 (D)
	0 : 0 : 10	1 : 3 : 4	315	60	hexagonal	plate	~11 (D)
	5 : 1 : 10	1 : 3 : 4	315	60	hexagonal	plate	~40 (D)
	5 : 1 : 100	1 : 3 : 4	315	60	hexagonal	flower	

A : Na(acac), B : $Y(acac)_3$, C : S, (D) : diameter

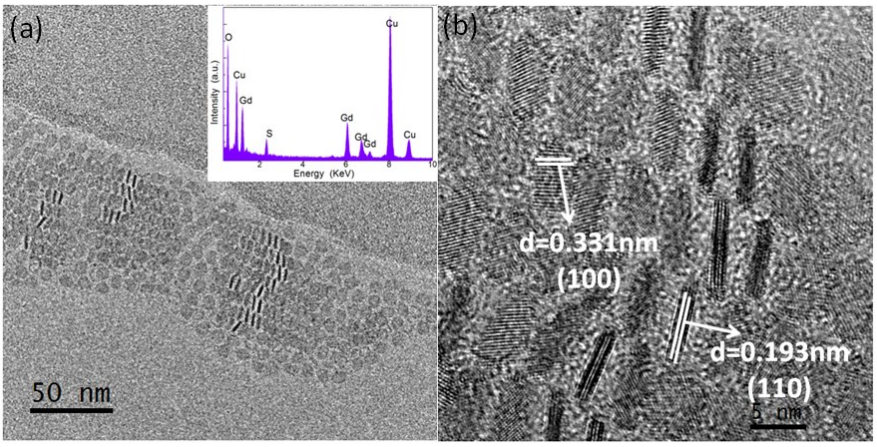

Figure S1 TEM (a) and HRTEM (b) images of Gd_2O_2S nanoplate with ~7nm in diameter. TEM specimens were dispersed in cyclohexane and ethanol mixture (cyclohexane : ethanol = 3:1) solution. Inset of (a) is the corrsponding EDS spectra.

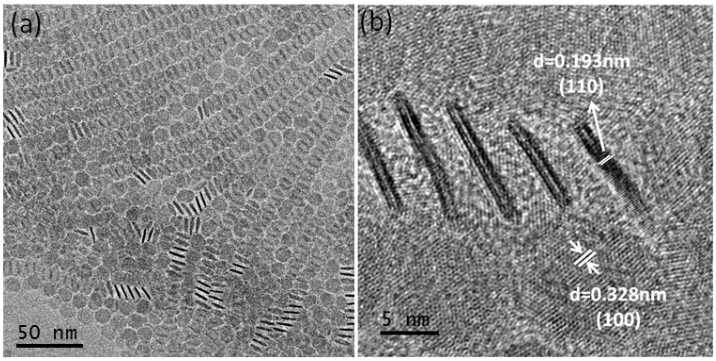

Figure S2 TEM and HRTEM images of Gd_2O_2S nanoplate prepared through taking the Gd_2O_2S nanoplate with ～7nm in diameter as seed. TEM specimens were dispersed in cyclohexane and ethanol mixture (cyclohexane : ethanol = 3:1) solution.

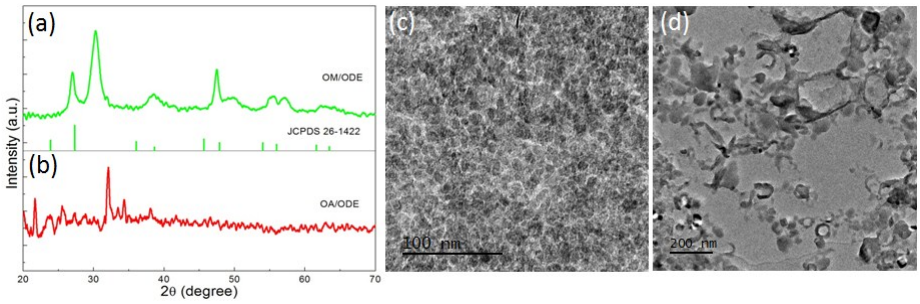

Figure S3 (a) XRD patterns of the products prepared under OM/ODE (a) and OA/ODE (b) solvent; (c) and (d) are the TEM images of (a) and (b).

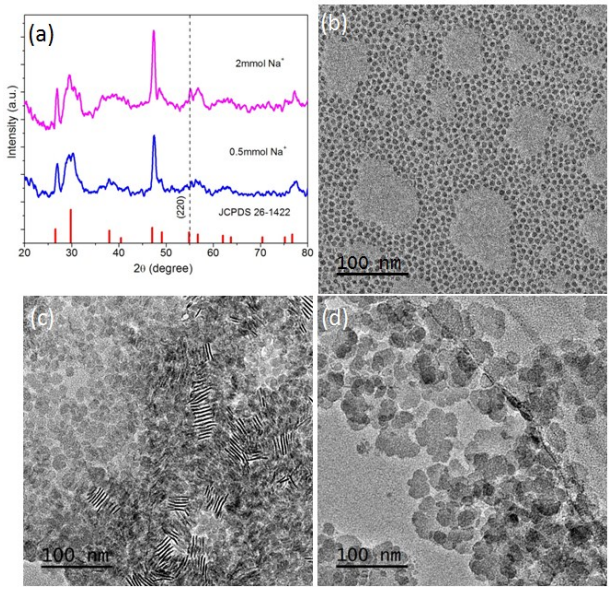

Figure S4 (a) XRD patterns of Gd_2O_2S NCs prepared with different Na^+ concentration (0.5, 2 mmol), bars represent standard hexagonal Gd_2O_2S crystal (JCPSD 26-1422) data; TEM images of Gd_2O_2S NCs prepared with different Na^+ concentration: (b) 0, (c) 0.5mmol, (d) 2mmol.

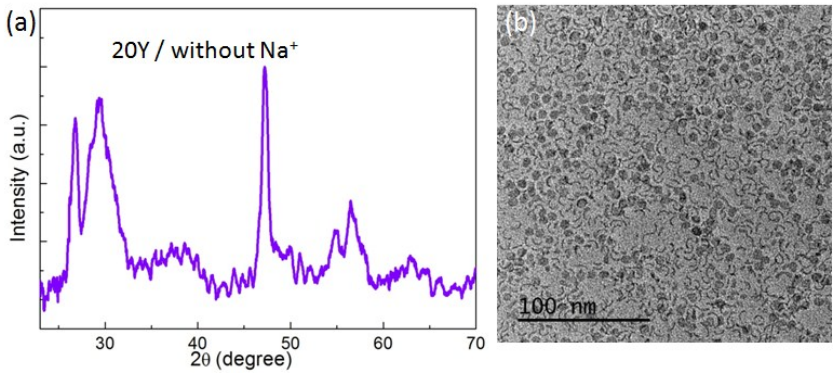

Figure S5 (a) XRD pattern of Gd_2O_2S NCs prepared with only doping Y^{3+} ions (20 mmol%), (b) TEM image of the corresponding Gd_2O_2S NCs.

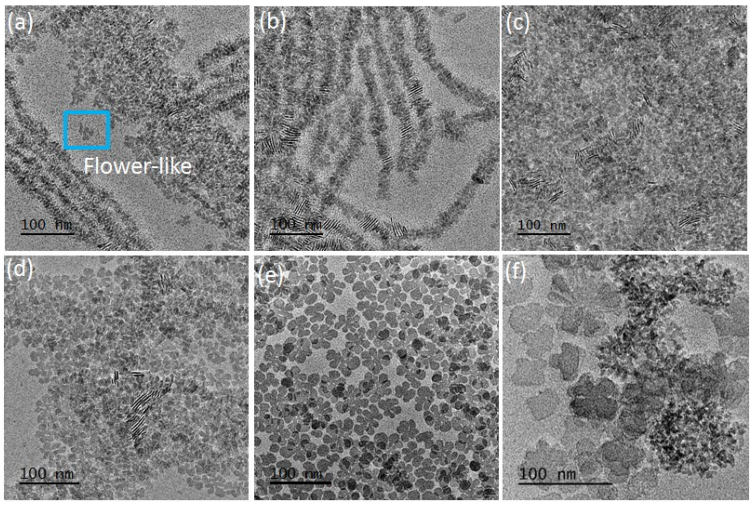

Figure S6 TEM images of the Gd_2O_2S NCs prepared under different reaction conditions: (a) 0min/315°C, (b) 2min/315°C, (c) 5min/315°C, (d) 10min/315°C, (e) 60min/315°C, (f) 60min/270°C.

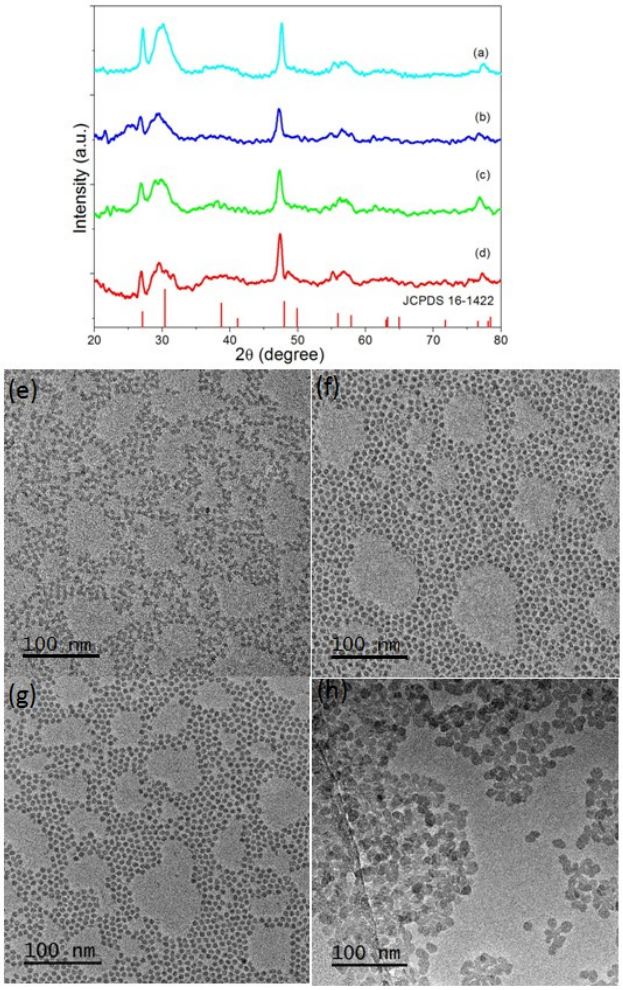

Figure S7 XRD patterns of Gd_2O_2S NCs prepared under different conditions: without Y^{3+}/Na^{+} and 1mmol S (a), 5 mmol S (b), 10 mmol S (c), with Y^{3+}/Na^{+} and 5mmol S (d); (e)-(h) are the corresponding TEM images of (a)-(d), respectively.

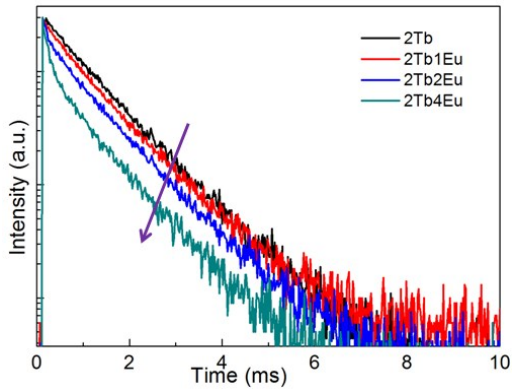

Figure S8 Decay curves of Tb^{3+}: $^5D_4$ level in F-NYG: 2%Tb/x%Eu (x=0, 1, 2, 4) samples.

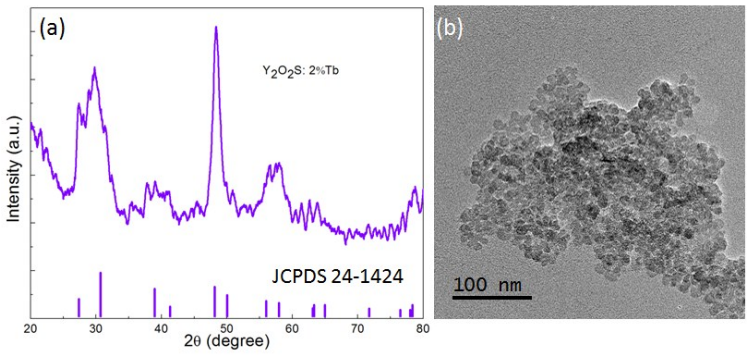

Figure S9 XRD pattern and TEM image of Y_2O_2S: 2%Tb NCs.

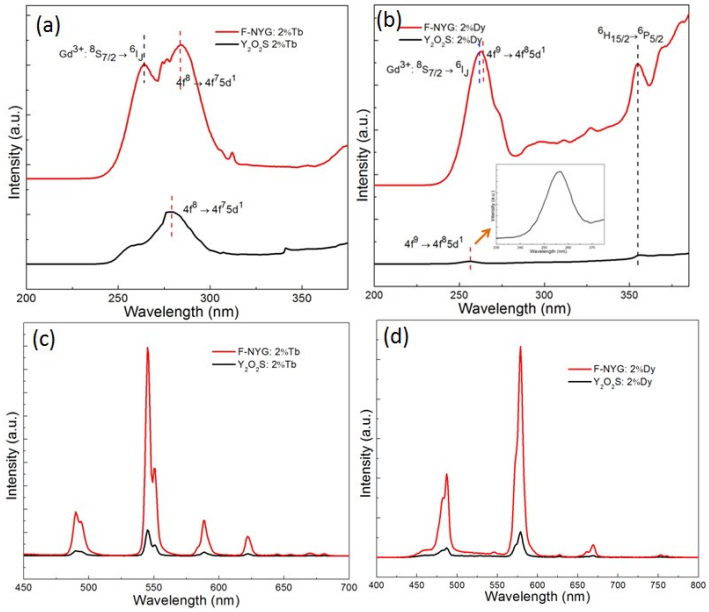

Figure S10 (a) and (b) are the PLE spectra of F-NYG: 2%Tb (Y_2O_2S: 2%Tb) and F-NYG: 2%Dy (Y_2O_2S: 2%Dy), respectively; (c) and (d) are the corresponding PL spectra.

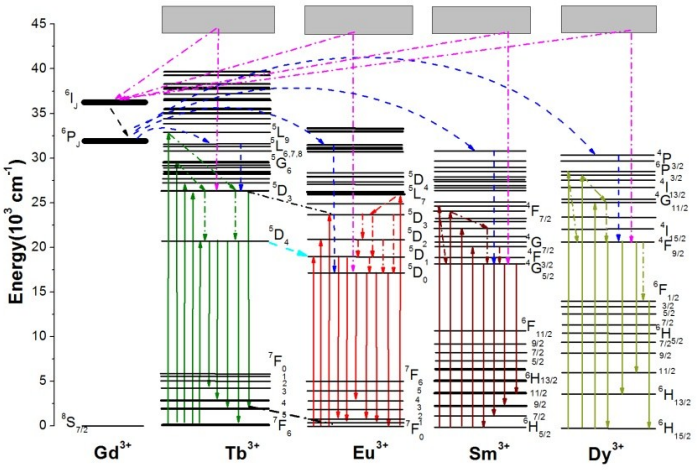

Figure S11 Schematic illustration of the energy transfer mechanism.

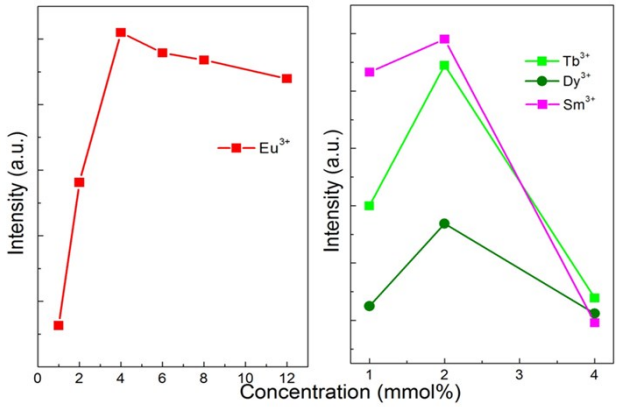

Figure S12 Dependence of the integral PL intensity on RE^{3+} (RE = Eu, Tb, Dy, Sm) concentration in F-NYG NCs.

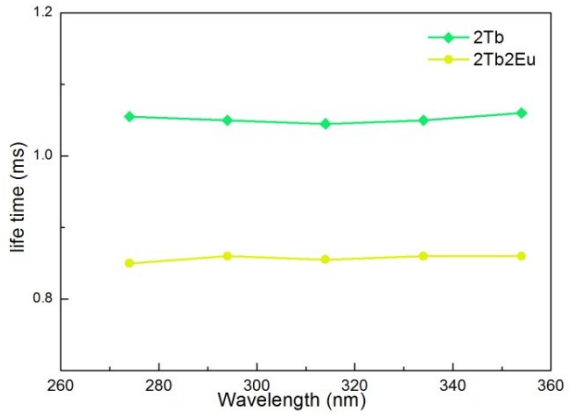

Figure S13 Life time of Tb^{3+}: $^5D_4$ level as a function of the excitation wavelength for F-NYG: 2%Tb and F-NYG: 2%Tb/2%Eu samples.

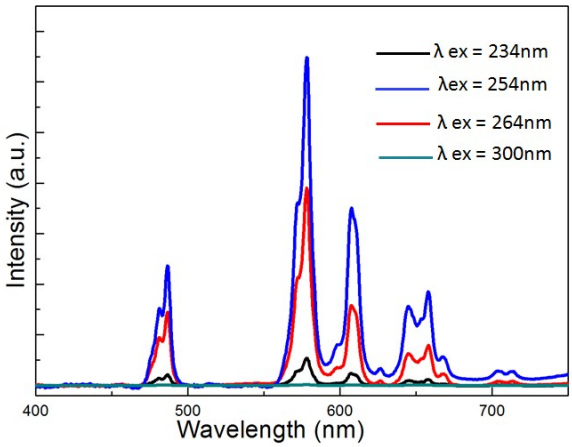

Figure S14 PL spectra of F-NYG: 1%Sm/2%Dy NCs under various excitation wavelengths.